DOI: 10.1002/chem.200802690

# A Binuclear $Cu^{II}$ Metallacycle Capable of Discerning between Pyrazine and Its Different Methyl-Substituted Derivatives Based on Reversible Intracage Metal–Ligand Binding

**Gui-Ge Hou, Jian-Ping Ma, Ting Sun, Yu-Bin Dong,* and Ru-Qi Huang[a]**

Metal-mediated self-assembly is an excellent approach to build up well-defined molecular containers with an isolated functional cavity that provide various functions such as molecular recognition, separation, and chemical reactions.[1] During recent decades, numerous self-assembled, metal-mediated, discrete molecular containers—in particular metallamacrocycles—have been reported.[2] Coordination-driven molecular containers with dynamically adjusting cavities in which the metal center acts as a reversible substrate-binding site, however, are rarely documented.[3] Metal-centered molecular containers with reversible binding sites for specific organic substrates might be metallaenzyme mimics. We have been interested in selective and reversible host–guest chemistry of metal-centered containers based on bent five-membered heteroatom ring-bridged organic ligands. Some of them display interesting selective, molecular recognizing, and tunable luminescent properties.[4] Herein, we present a preliminary report on a $Cu^{II}$–macrocycle formed by a simple self-assembly process working as a highly selective host cage for reversible encapsulation of pyrazine and its different methyl-substituted derivatives through metal–ligand interactions. More importantly, it is capable of discerning between pyrazine molecules that have different numbers of methyl substituents.

Metalation of ligand LH with $Cu(OAc)_2$ in an EtOH/THF mixed solvent system at room temperature afforded the neutral metallamacrocyclic complex $\{Cu_2L_2\}_n$. The coordination geometry around the $Cu^{II}$ center is square planar with an $N_2O_2$ donor environment (Scheme 1). The opposite Cu···Cu and O···O distances in the $Cu_2L_2$ unit are 8.8 and 8.4 Å, respectively. In addition, the four exocyclic pyridyls surround the ring and spread effectively outside, thus making a saddle-shaped cage. These $Cu_2L_2$ rings are weakly linked together through four equivalent exocyclic Cu–N bonds into a 3D framework. The external pyridine–copper distance is 2.376(5) Å, which is longer than the Cu–N (apical pyridine) bond length of 2.10–2.20 Å commonly observed in $Cu^{II}$ complexes. This makes the externally bound pyridine donors particularly labile, especially in solution.[5] Two such identical frameworks interpenetrate each other to generate a high density structure (see the Supporting Information).

The crystals of **1** are not soluble in DMSO or DMF, are sparingly soluble in MeOH, but are soluble in $CHCl_3$. The ESIMS of **1** shows a prominent signal at $m/z$ 1207 (see the Supporting Information), indicating the formation of the neutral, discrete $Cu_2L_2$ (**2**) molecular cage in solution. Cage **2** has two square-planar $Cu^{II}$ centers separated by 8.8 Å, which hopefully form a perfect host pocket to trap pyrazine (N···N separation of approximately 2.8 Å) and its derivatives by weakly coordinating interactions. This is because a $Cu^{II}$ ion can adopt a square-pyramidal coordination sphere and a size matching between the pyrazine guest and the $Cu_2L_2$ host. Indeed, when **2** was treated with an excess of pyrazine in $CHCl_3$/DMF at room temperature, the new host–guest system $Cu_2L_2$(pyrazine)·5$CHCl_3$ (**3**) was generated in high yield, and was confirmed by single-crystal X-ray analysis. Compound **3** crystallizes in the triclinic space group $P\bar{1}$. As shown in Figure 1, the trapped pyrazine molecule is centered in the $Cu_2L_2$ pocket and weakly coordinates to the $Cu^{II}$ centers. The bond length between the copper and pyrazine nitrogen (Cu1–N3) is 2.409 Å, even longer than that of **1**, but within the range of 2.6–2.8 Å for axial Cu–N bond lengths.[6] In the solid state, the $Cu_2L_2$ rings stack together along the crystallographic $c$ axis to generate columns with squarelike channels in which the pyrazine guests arrange in parallel (Figure 1). No intermolecular π–π interactions have

[a] G.-G. Hou, J.-P. Ma, T. Sun, Prof. Dr. Y.-B. Dong, Prof. R.-Q. Huang
College of Chemistry, Chemical Engineering and Materials Science
Key Lab of Molecular and Nano Probes
Engineering Research Center of Pesticide and
Medicine Intermediate Clean Production
Ministry of Education, Shandong Normal University
Jinan, 250014 (P.R. China)
Fax: (+86) 531-82615258
E-mail: yubindong@sdnu.edu.cn

Supporting information for this article is available on the WWW under http://dx.doi.org/10.1002/chem.200802690.

   

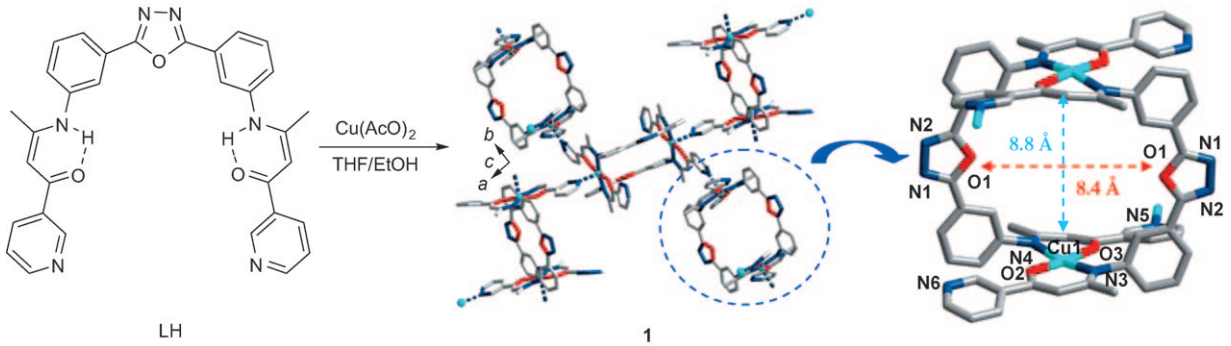


Scheme 1. The synthesis of **1**. The long external cage pyridine–copper distances are shown as dotted lines.

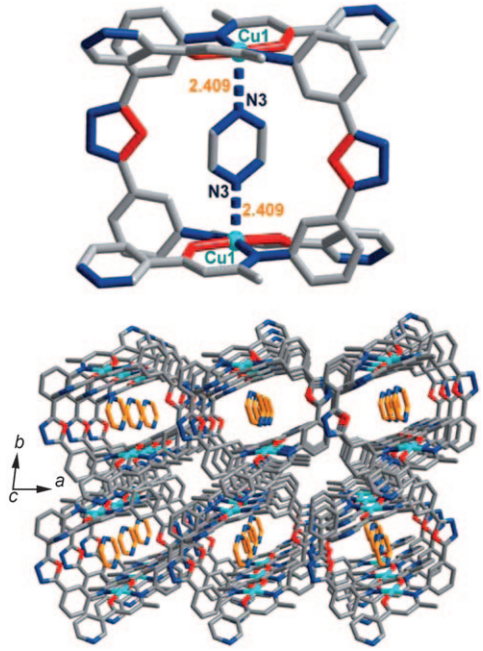


Figure 1. Top: molecular structures of **3**; the weak Cu–N coordination interactions are shown as dotted lines. Bottom: crystal packing of **3**; the trapped pyrazine is shown in orange for clarity.

been found in **3**. The $Cu^{II}\cdots Cu^{II}$ separation in **3** is 7.6 Å, which has contracted by 1.2 Å compared with that of the hollow cage, whereas the opposite oxadiazole O3···O3 distance is 8.8 Å, which has expanded by 0.4 Å compared with that of the hollow cage.

A host cage that could bind a guest moiety in a reversible fashion would lead to practical applications. As shown in Figure 1, the effective pores in the extended structure, and the weak $Cu^{II}$–pyrazine interaction, would allow easy mobility of the pyrazine guests through the crystal in a reversible manner. Indeed, the pyrazine molecules included in the pores could be readily removed by solid–liquid extractions. When the crystalline solid of **3** was stirred in $[D_6]$DMSO at room temperature for approximately one day (monitored by $^1$H NMR spectroscopy), the weakly coordinated pyrazine guests were removed by extraction with $[D_6]$DMSO. The powder XRD pattern of the hollow cage has sharp diffraction peaks, indicating that the ring structure is maintained without the pyrazine guest, but undergoes a slight change compared with that of the initial framework of **3** (Figure 2a,b). The ESIMS (see the Supporting Information) spectrum, $^1$H NMR spectrum, and elemental analysis indicate that the hollow cage of **2** was regenerated (see Figure 2b for powder XRD pattern and $^1$H NMR spectrum of **2**). Furthermore, when the regenerated **2** was suspended in a solution of pyrazine (excess) in $[D_6]$DMSO at room temperature, the pyrazine guests are reincorporated into the cage. The powder XRD pattern indicates that the pyrazine⊂$Cu_2L_2$ species is completely reformed (Figure 2c). Compound **2** is

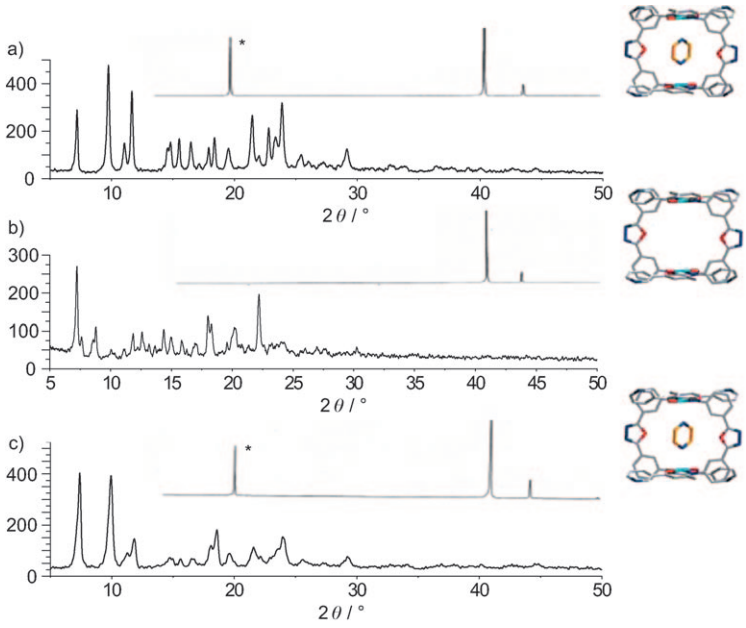


Figure 2. a) The powder XRD pattern of **3** and the $^1$H NMR spectrum obtained from the $[D_6]$DMSO extract, b) the powder XRD pattern of the hollow cage and the $^1$H NMR spectrum obtained from the $[D_6]$DMSO extract, and c) the powder XRD pattern of regenerated **3** and the $^1$H NMR spectrum obtained from the $[D_6]$DMSO extract. The signals marked by an asterisk correspond to the pyrazine protons ($\delta = 8.65$ ppm).

  

insoluble in DMSO, therefore, it is unlikely that a dissolution–recrystallization mechanism could explain the pyrazine reabsorption.

It is also notable that the $Cu_2L_2$ hollow cage can reversibly absorb and reabsorb 2-methylpyrazine and 2,5-dimethylpyrazine guests under the same reaction conditions. The crystal structures (Figure 3) revealed that compound **4** ($Cu_2L_2$(2-methylpyrazine)·2.5$CHCl_3$) crystallizes in the triclinic system $P\bar{1}$, whereas compound **5** ($Cu_2L_2$(2,5-dimethylpyrazine)·3$CHCl_3$ crystallizes in the triclinic system $P\bar{1}$ (**5a**, major) and the monoclinic system $P2(1)$ (**5b**, minor), respectively. Notably, products **5a** and **5b** are the same 2,5-dimethylpyrazine⊂$Cu_2L_2$ host–guest complexes and exhibit similar solid-state arrangements (see the Supporting Information). The Cu–N bond lengths in **4** and **5** are in the range of 2.496(4) to 2.665(6) Å, which are significantly longer than that of **3**. The $Cu^{II}\cdots Cu^{II}$ distances in **4** and **5** are 7.8 and 7.9 Å, respectively, whereas the distance between the two opposite oxadiazole oxygen atoms are 8.7 and 8.9 Å, respectively. Compared with **3**, all of the changes that occur in **4**–**5** are clearly because of the steric demands resulting from the substituted methyl groups on the pyrazinyl ring. Thus, the $Cu_2L_2$ cage in compounds **4** and **5** is a flexible, spongelike, and dynamic framework that can adjust its internal space in response to different guest molecules.[4a,7] It is different from the $Cu_2L_2$ cage in **3** because the weak intermolecular π–π interactions exist in **4** and **5** in the solid state. Each neutral ring in **4** and **5** stacks on its neighbors through the central oxadiazole moiety along the channel direction, which generates a π–π-sustained two-dimensional network containing squarelike channels in which the methyl-substituted pyridine guest molecules are located (Figure 3). However, the hollow $Cu_2L_2$ cage does not respond to the other pyrazine derivatives, such as 2,3-dimethylpyrazine, 2,6-dimethylpyrazine, 2,3,5,6-tetramethylpyridine, and benzo[α]-pyrazine, under the experimental conditions, which is clearly caused by the steric repulsion of the substituted groups adjacent to the nitrogen donors.

The major hurdle in molecular recognition is selectivity, that is, preparing a host pocket that responds only to the specific substrate in the presence of other different potential competitors. To explore the molecular selectivity of the hollow cage **2**, its binding affinity for pyrazine, 2-methylpyrazine, and 2,5-dimethylpyrazine was examined. When **2** was treated with a mixture of pyrazine, 2-methylpyrazine, and 2,5-dimethylpyrazine (molar ratio: 2-pyrazine/2-methylpyrazine/2,5-dimethylpyrazine 1:20:20:20) in a $CHCl_3$/DMF mixed solvent system at room temperature, only **3** was formed, which is confirmed by single-crystal X-ray analysis and $^1$H NMR spectroscopy of the [$D_6$]DMSO extract of the resulting crystals (see the Supporting Information). Moreover, when **2** was treated with 2-methylpyrazine and 2,5-dimethylpyrazine in a molar ratio of 1:20:20, only compound **5** was obtained, which was confirmed by single-crystal X-ray analysis and $^1$H NMR spectroscopy of the [$D_6$]DMSO extract of the resulting crystals (see the Supporting Information). Thus, of the three types of guests, guest **2** has the best binding affinity for pyrazine and the poorest affinity for 2-methylpyrazine under the experimental conditions. To date, only a handful of metal-centered molecular containers with reversible binding sites[3c] and dynamically adjustable cavities for specific organic substrates have been presented.

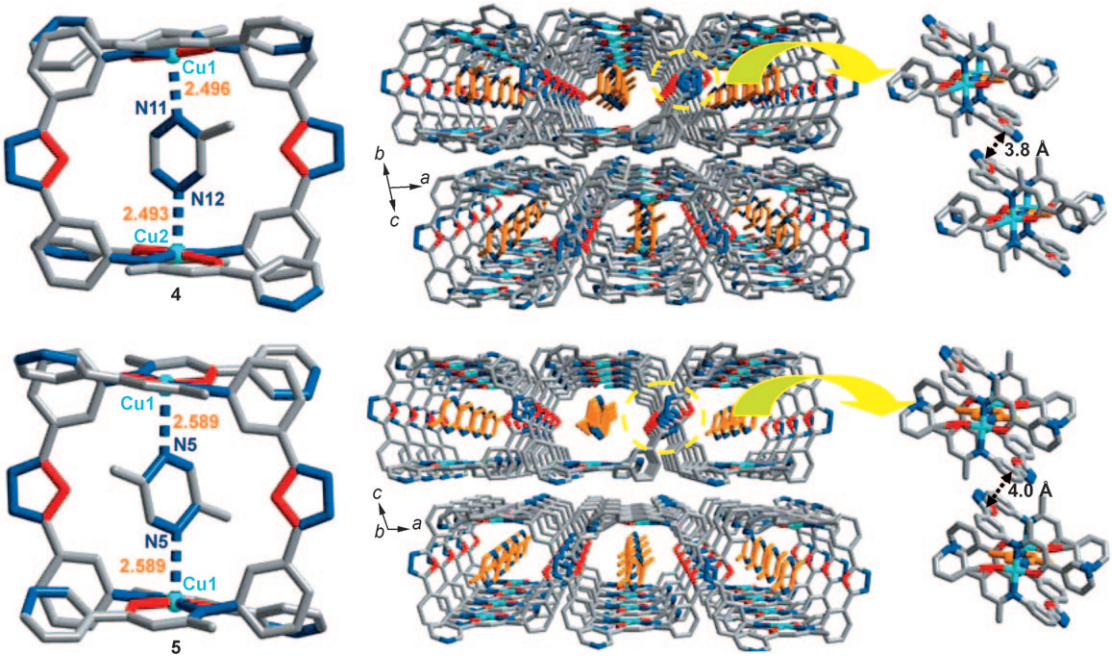


Figure 3. Molecular structures and solid-state packing of **4** (top) and **5** (bottom). Hydrogen atoms and solvent molecules of crystallization are omitted for clarity. For **5**, only the structure of major product **5a** is shown. The molecular structure and solid-state packing of **5b** are given in the Supporting Information.

  

More importantly, the study of the molecular-recognizing ability of **2** was simultaneously performed in the presence of the similar competitors instead of by a respective detection observed in previous studies.[3c,8] To the best of our knowledge, cage **2** is the first "breathing" discrete metallamacrocycle that is able to recognize specific substrates in the presence of other competitors by means of the internal space based on its reversible metal-binding property.

In summary, a reversible spongelike $M_2L_2$ molecular cage with extreme sensitivity and selectivity towards pyrazine and different methyl-substituted derivatives has been reported. Such materials may find applications in the fields of separation, sensors, and purification, and studies towards the preparation of new discrete and polymeric "breathing" molecular cages based on other bent heterocycle-bridged organic ligands of this type. Heterometallic coordination complexes based on these are currently under investigation.

## Experimental Section

**Synthesis of LH**: 2,5-Bis(3-aminobenzoyl)-1,3,4-oxadiazole (1.0 g, 3.97 mmol) and nicotinoylacetone (2.5 g, 15.34 mmol) in an EtOH/HCOOH (30 mL/0.2 mL) system was heated to reflux for 30 h to generate LH as a yellow crystalline solid (1.1 g, 51% yield). M.p. 248–250°C; $^1$H NMR (300 MHz, $CDCl_3$, 25°C, TMS): $\delta$ = 13.25 (s, 2H; -OH), 9.14 (s, 2H; -$C_5H_4N$), 8.71 (d, 2H; -$C_5H_4N$), 8.25 (d, 2H; -$C_5H_4N$), 8.04 (d, 2H; -$C_6H_4$), 7.99 (s, 2H; -$C_5H_4N$), 7.59 (t, 2H; -$C_6H_4$), 7.42 (m, 4H; -$C_6H_4$), 5.95 (s, 2H; -CH=C-), 2.26 (s, 3H; -$CH_3$), 1.43 ppm (s, 3H; -$CH_3$); IR (KBr): 3443 (s), 1584 (s), 1547 (s), 1472 (m), 1520 (m), 1410 (m), 1328 (s), 1297 (s), 1195 (s), 1095 (s), 1024 (s), 895 (m), 1024 (s), 768 (s), 687 cm$^{-1}$ (m); elemental analysis calcd (%) for $C_{32}H_{26}N_6O_3$: C 70.85, H 4.80, N 15.50; found: C 70.92, H 4.75, N 15.45.

**Synthesis of $Cu_2L_2$ (1) and (2)**: $Cu(AcO)_2{\cdot}6H_2O$ (8.0 mg, 0.04 mmol) in EtOH (8 mL) was layered onto a solution of L (22 mg, 0.04 mmol) in THF (8 mL). The solutions were left for approximately one week at room temperature, and green/black crystals were obtained (21.8 mg, 78% yield; based on $Cu(AcO)_2{\cdot}6H_2O$). IR (KBr): 3441 (s), 1588 (s), 1556 (m), 1507 (s), 1474 (s), 1446 (s), 1397 (s), 1293 (m), 1207 (m), 1025 (m), 869 (m), 728 cm$^{-1}$ (m); elemental analysis calcd (%) for $C_{64}H_{48}Cu_2N_{12}O_6$: C 63.58, H 3.97, N 13.91; found: C 63.65, H 3.85, N 13.76. When **1** was dissolved in $CHCl_3$, the discrete $Cu_2L_2$ compound of **2** was obtained. ESIMS: $m/z$ 1207 $[C_{64}H_{48}Cu_2N_{12}O_6+1]^+$.

**Synthesis of [$Cu_2L_2$(pyrazine)]·5 $CHCl_3$ (3)**: DMF (2 mL) was carefully layered onto a solution of **2** (6.0 mg, 0.005 mmol) and pyrazine (8 mg, 0.100 mmol) in $CHCl_3$ (2 mL). The solutions were left for approximately 3 days at room temperature, and deep-green crystals were obtained (5.2 mg, 70% yield; based on **2**). IR (KBr): 3441 (m), 1588 (s), 1555 (s), 1516 (s), 1472 (s), 1448 (s), 1400 (s), 1293 (m), 1206 (m), 1027 (m), 866 (m), 747 (m), 698 cm$^{-1}$ (m). The crystals obtained desolvate rapidly and lose crystallinity upon isolation. The elemental analysis corresponds to the formula [$Cu_2L_2$(pyrazine)]. Elemental analysis calcd (%) for $C_{68}H_{52}Cu_2N_{14}O_6$: C 63.39, H 4.07, N 15.22; found: C 63.16, H 4.15, N 15.44.

**Synthesis of [$Cu_2L_2$(2-methylpyrazine)]·2.5 $CHCl_3$ (4)**: DMF (2 mL) was carefully layered onto a solution of **2** (6.0 mg, 0.005 mmol) and 2-methylpyrazine (9 mg, 0.100 mmol) in $CHCl_3$ (2 mL). The solutions were left for approximately 7 days at room temperature, and deep-green crystals were obtained (4.8 mg, 60% yield; based on **2**). IR (KBr): 3445 (m), 1587 (s), 1555 (s), 1505 (s), 1446 (s), 1293 (m), 1207 (m), 1122 (m), 1064 (m), 1024 (m), 901 (m), 866 (m), 849 (m), 798 (m), 751 (m), 721 (m), 699 (m), 577 cm$^{-1}$ (m). The crystals desolvate rapidly and lose crystallinity upon isolation. The elemental analysis corresponds to the formula [$Cu_2L_2$(2-methylpyrazine)]. Elemental analysis calcd (%) for $C_{69}H_{54}Cu_2N_{14}O_6$: C 63.63, H 4.18, N 15.06; found: C 63.38, H 4.32, N 15.24.

**Synthesis of [$Cu_2L_2$(2,5-dimethylpyrazine)]·3 $CHCl_3$ (5)**: DMF (2 mL) was carefully layered onto a solution of **2** (6.0 mg, 0.005 mmol) and 2,5-dimethylpyrazine (10 mg, 0.100 mmol) in $CHCl_3$ (2 mL). The solutions were left for approximately 7 days at room temperature, and deep-green blocklike (**5a**; 4.2 mg, 50% yield) and platelike (**5b**; 0.06 mg, 7% yield) crystals were obtained. Single-crystal X-ray analysis revealed that **5a** and **5b** are isomeric. IR (KBr): 3421 (m), 1588 (s), 1557 (s), 1508 (s), 1473 (s), 1445 (s), 1397 (s), 1294 (m), 1207 (m), 1123 (m), 1026 (m), 898 (m), 868 (m), 802 (m), 751 (m), 724 (m), 699 (m), 581 cm$^{-1}$ (m). The crystals desolvate rapidly and lose crystallinity upon isolation. The elemental analysis corresponds to the formula [$Cu_2L_2$(2,5-dimethylpyrazine)]. Elemental analysis calcd (%) for $C_{70}H_{56}Cu_2N_{14}O_6$: C 63.87, H 4.29, N 14.90; found: C 63.68, H 4.36, N 14.72.

**Crystal data for LH**: $C_{32}H_{26}N_6O_3$; monoclinic; $P2/n$; $M_r$ = 542.59; $a$ = 10.979(3), $b$ = 6.0754(17), $c$ = 19.843(5) Å; $\beta$ = 98.732(4)°; $V$ = 1308.2(6) Å$^3$; $Z$ = 2; $\rho_{calcd}$ = 1.377 g cm$^{-3}$; $\mu(Mo_{K\alpha})$ = 0.582 mm$^{-1}$; $F(000)$ = 568; $T$ = 298(2) K; $\lambda(Mo_{K\alpha})$ = 0.71073 Å; $\theta_{max}$ = 25.03°; reflections collected/unique: 5001/2306 [$R_{int}$ = 0.0404]; $R_1$ ($I > 2\sigma(I)$) = 0.0482; $wR_2$ ($I > 2\sigma(I)$) = 0.1060.

**Crystal data for 1**: $C_{64}H_{48}Cu_2N_{12}O_6$; tetragonal; $P4(2)/n$; $M_r$ = 1208.22; $a$ = 22.7841(16), $b$ = 22.7841(16), $c$ = 15.297(2) Å; $V$ = 7940.7(13) Å$^3$; $Z$ = 4, $\rho_{calcd}$ = 1.011 g cm$^{-3}$; $\mu(Mo_{K\alpha})$ = 0.582 mm$^{-1}$; $F(000)$ = 2488; $T$ = 298(2) K; $\lambda(Mo_{K\alpha})$ = 0.71073 Å; $\theta_{max}$ = 25.01°; reflections collected/unique: 40845/6983 [$R_{int}$ = 0.1270]; $R_1$ ($I > 2\sigma(I)$) = 0.0729; $wR_2$ ($I > 2\sigma(I)$) = 0.1578.

**Crystal data for 3**: $C_{73}H_{57}Cl_{15}Cu_2N_{14}O_6$; triclinic; $P\bar{1}$; $M_r$ = 1885.16; $a$ = 12.0892(19), $b$ = 12.875(2), $c$ = 13.976(2) Å; $\alpha$ = 71.030(2), $\beta$ = 77.030(2), $\gamma$ = 79.031(2)°; $V$ = 1988.3(5) Å$^3$; $Z$ = 1; $\rho_{calcd}$ = 1.574 g cm$^{-3}$; $\mu(Mo_{K\alpha})$ = 1.100 mm$^{-1}$; $F(000)$ = 954; $T$ = 174(2) K; $\lambda(Mo_{K\alpha})$ = 0.71073 Å; $\theta_{max}$ = 25.50°; reflections collected/unique: 9999/7255 [$R_{int}$ = 0.0220]; $R_1$ ($I > 2\sigma(I)$) = 0.0748; $wR_2$ ($I > 2\sigma(I)$) = 0.1848.

**Crystal data for 4**: $C_{71.50}H_{56.50}Cl_{7.50}Cu_2N_{14}O_6$; triclinic; $P\bar{1}$; $M_r$ = 1600.76; $a$ = 12.2525(18), $b$ = 17.680(2), $c$ = 17.895(3) Å; $\alpha$ = 92.546(2), $\beta$ = 91.384(2), $\gamma$ = 108.507(2)°; $V$ = 3669.4(9) Å$^3$; $Z$ = 2; $\rho_{calcd}$ = 1.449 g cm$^{-3}$; $\mu(Mo_{K\alpha})$ = 0.914 mm$^{-1}$; $F(000)$ = 1634; $T$ = 298(2) K; $\lambda(Mo_{K\alpha})$ = 0.71073 Å; $\theta_{max}$ = 25.50°; reflections collected/unique: 19286/13386 [$R_{int}$ = 0.0242]; $R_1$ ($I > 2\sigma(I)$) = 0.0644; $wR_2$ ($I > 2\sigma(I)$) = 0.1828.

**Crystal data for 5**: **5a**: $C_{73}H_{59}Cl_9Cu_2N_{14}O_6$; triclinic; $P\bar{1}$; $M_r$ = 1674.47; $a$ = 12.316(5), $b$ = 12.411(5), $c$ = 13.015(5) Å; $\alpha$ = 91.797(5), $\beta$ = 103.385(5), $\gamma$ = 104.398(5)°; $V$ = 1866.2(12) Å$^3$; $Z$ = 1; $\rho_{calcd}$ = 1.490 g cm$^{-3}$; $\mu(Mo_{K\alpha})$ = 0.954 mm$^{-1}$; $F(000)$ = 854; $T$ = 173(2) K; $\lambda(Mo_{K\alpha})$ = 0.71073 Å; $\theta_{max}$ = 25.35°; reflections collected/unique: 9492/6650 [$R_{int}$ = 0.0426]; $R_1$ ($I > 2\sigma(I)$) = 0.0927; $wR_2$ ($I > 2\sigma(I)$) = 0.2380. **5b**: $C_{73}H_{59}Cl_9Cu_2N_{14}O_6$; monoclinic; $P2(1)$; $M_r$ = 1674.47; $a$ = 12.227(3), $b$ = 24.892(6), $c$ = 12.577(3) Å; $\beta$ = 105.640(5)°; $V$ = 3686.1(15) Å$^3$; $Z$ = 1; $\rho_{calcd}$ = 1.509 g cm$^{-3}$; $\mu(Mo_{K\alpha})$ = 0.966 mm$^{-1}$; $F(000)$ = 1708; $T$ = 173(2) K; $\lambda(Mo_{K\alpha})$ = 0.71073 Å; $\theta_{max}$ = 25.01°; reflections collected/unique: 18721/12578 [$R_{int}$ = 0.0811]; $R_1$ ($I > 2\sigma(I)$) = 0.0878; $wR_2$ ($I > 2\sigma(I)$) = 0.1439.

CCDC-693335 (**1**), 693336 (**3**), 693337 (**4**), 693338 (**5a**), 700878 (**5b**), 700879 (**3′**), 700880 (**5a′**), and 700881 (**5b′**) contain the supplementary crystallographic data for this paper. These data can be obtained free of charge from The Cambridge Crystallographic Data Centre via www.ccdc.cam.ac.uk/data_request/cif

## Acknowledgements

We are grateful for financial support from the National Natural Science Foundation of China (grant nos. 20871076 and 20671060), Shangdong Natural Science Foundation (grant no. JQ200803), and the Ph.D. Programs Foundation of the Ministry of Education of China (grant no. 200804450001).

  

**Keywords:** copper · host–guest systems · molecular recognition · oxadiazole · pyrazine

[1] a) S. Leininger, B. Olenyuk, P. J. Stang, *Chem. Rev.* **2000**, *100*, 853; b) M. Fujita, K. Umemoto, M. Yoshizawa, N. Fujita, T. Kusukawa, K. Biradha, *Chem. Commun.* **2001**, 509; c) D. L. Caulder, K. N. Raymond, *Acc. Chem. Res.* **1999**, *32*, 975.

[2] For some examples of metallacycles, see: a) S. Masaoka, S. Furukawa, H.-C. Chang, T. Mizutani, S. Kitagawa, *Angew. Chem.* **2001**, *113*, 3933; *Angew. Chem. Int. Ed.* **2001**, *40*, 3817; b) V. C. Lau, L. A. Berben, J. R. Long, *J. Am. Chem. Soc.* **2002**, *124*, 9042; c) S. J. Lee, W. Lin, *J. Am. Chem. Soc.* **2002**, *124*, 4554; d) A. Hori, K. Yamashita, M. Fujita, *Angew. Chem.* **2004**, *116*, 5126; *Angew. Chem. Int. Ed.* **2004**, *43*, 5016; e) P. H. Dinolfo, M. E. Williams, C. L. Stern, J. T. Hupp, *J. Am. Chem. Soc.* **2004**, *126*, 12989; f) S. B. Zhao, R. Y. Wang, S. Wang, *J. Am. Chem. Soc.* **2007**, *129*, 3092; g) R. W. Saalfrank, A. Scheurer, R. Puchta, F. Hampel, H. Maid, F. W. Heinemann, *Angew. Chem.* **2007**, *119*, 269; *Angew. Chem. Int. Ed.* **2007**, *46*, 265.

[3] a) K.-H. Kim, R. Song, K. M. Kim, *J. Am. Chem. Soc.* **2003**, *125*, 7170; b) N. P. Power, S. J. Dalgarno, J. L. Atwood, *Angew. Chem.* **2007**, *119*, 8755; *Angew. Chem. Int. Ed.* **2007**, *46*, 8601; c) K.-H. Kim, R. Song, K. M. Kim, *J. Am. Chem. Soc.* **2003**, *125*, 7170.

[4] a) Y.-B. Dong, Q. Zhang, L.-L. Liu, J.-P. Ma, B. Tang, R.-Q. Huang, *J. Am. Chem. Soc.* **2007**, *129*, 1514; b) Y.-B. Dong, P. Wang, J.-P. Ma, X.-X. Zhao, B. Tang, R.-Q. Huang, *J. Am. Chem. Soc.* **2007**, *129*, 4872; c) P. Wang, J.-P. Ma, Y.-B. Dong, R.-Q. Huang, *J. Am. Chem. Soc.* **2007**, *129*, 10620.

[5] M. A. Alam, M. Nethaji, M. Ray, *Angew. Chem.* **2003**, *115*, 1984; *Angew. Chem. Int. Ed.* **2003**, *42*, 1940.

[6] Tables of Interatomic Distances and Configuration in Molecules and Ions, *Chem. Soc., Special Publ. No. 11*, **1958**.

[7] a) S. Kitagawa, K. Uemura, *Chem. Soc. Rev.* **2005**, *34*, 109; b) F. Millange, C. Serre, N. Férey, G. Guillou, R. I. Walton, *Angew. Chem.* **2008**, *120*, 4168; *Angew. Chem. Int. Ed.* **2008**, *47*, 4100; c) P. L. Llewellyn, G. Maurin, T. Devic, S. Loera-Serna, N. Rosenbach, C. Serre, S. Bourelly, P. Horcajada, Y. Filinchuk, G. Férey, *J. Am. Chem. Soc.* **2008**, *130*, 12808.

[8] A. W. Maverick, M. L. Ivie, J. H. Waggenspack, F. R. Fronczek, *Inorg. Chem.* **1990**, *29*, 2403.

Received: December 19, 2008
Published online: January 29, 2009

  